Observations of planetary heating since the 1980s from multiple independent datasets

Allison, L. C. ORCID: https://orcid.org/0000-0002-9271-1197, Palmer, M. D. ORCID: https://orcid.org/0000-0001-7422-198X, Allan, R. ORCID: https://orcid.org/0000-0003-0264-9447, Hermanson, L. ORCID: https://orcid.org/0000-0002-1062-6731, Liu, C. ORCID: https://orcid.org/0000-0002-6663-452X and Smith, D. M. ORCID: https://orcid.org/0000-0001-5708-694X (2020) Observations of planetary heating since the 1980s from multiple independent datasets. Environmental Research Communications, 2 (10). p. 101001. ISSN 2515-7620 doi: https://doi.org/10.1088/2515-7620/abbb39 Available at http://centaur.reading.ac.uk/93369/

Observations of planetary heating since the 1980s from multiple independent datasets

Environmental Research Communications

LETTER

Observations of planetary heating since the 1980s from multiple independent datasets

Lesley C Allison[1], Matthew D Palmer[1], Richard P Allan[2], Leon Hermanson[1], Chunlei Liu[2,3] and Doug M Smith[1]

[1] Met Office Hadley Centre, Exeter, United Kingdom
[2] Department of Meteorology and National Centre for Earth Observation, University of Reading, Reading, United Kingdom
[3] SIMM, Guangdong Ocean University, Zhanjiang, People's Republic of China

E-mail: lesley.allison@metoffice.gov.uk

OPEN ACCESS

RECEIVED
15 June 2020

REVISED
12 September 2020

ACCEPTED FOR PUBLICATION
24 September 2020

PUBLISHED
5 October 2020

Abstract

Time series of global mean surface temperature are widely used to measure the rate of climate change that results from Earth's energy imbalance. However, studies based on climate model simulations suggest that on annual-to-decadal timescales global ocean heat content is a more reliable indicator. Here we examine the observational evidence for this, drawing together multiple datasets that span the past ~30 years. This observational analysis strongly supports the model-based finding that global ocean heat content and sea level are more reliable than surface temperature for monitoring Earth's energy accumulation on these timescales. Global ocean temperature anomalies in the 0–100 m and 100–250 m layers are negatively correlated ($r = -0.36$), primarily explained by the influence of the Tropical Pacific, and a clearer heating signal is revealed by integrating over deeper ocean layers. The striking agreement between multiple independent datasets represents unequivocal evidence of ongoing planetary heating.

Introduction

Greenhouse gas emissions have caused a persistent radiative imbalance at the top of the atmosphere (TOA), referred to as Earth's energy imbalance (EEI), resulting in ongoing planetary heating that is driving the various facets of observed climate change (von Schuckmann *et al* 2016). Time series of global mean surface temperature (GMST) are widely used to quantify the rate of anthropogenic climate change and to define warming targets for policy discussions. However, GMST is strongly influenced by internal variability and its decadal trends do not always reflect the underlying long-term warming, for example during the recent 'hiatus' period where temperature rise stalled despite strong evidence of sustained planetary heating associated with greenhouse gas forcing (e.g. England *et al* 2014, Medhaug *et al* 2017; figure 1). More than 90% of the multi-decadal EEI is manifested in global ocean heat content (GOHC) gain (von Schuckmann *et al* 2016). Climate model evidence suggests that on decadal timescales GOHC provides a more robust measure of EEI than GMST does (Palmer *et al* 2011, Palmer and McNeall 2014). But what is the observational evidence for this? Studies that examined a recent decade of improved ocean observations (2005–2015) showed that year-to-year variations in GOHC agree well with independent measurements of TOA radiances, promoting confidence in our ability to observe variations in EEI at sub-decadal timescales (Johnson *et al* 2016) and, in contrast to the variable surface temperature record, the global sub-surface ocean (300–2000m) warmed steadily over this period (Wijffels *et al* 2016, Cheng *et al* 2017a). Here we examine EEI over a longer time horizon (~30 years) and make use of new reconstructions of accumulated TOA flux and global mean sea level (GMSL) alongside GMST and GOHC estimates to explore the agreement between these independent observational datasets.

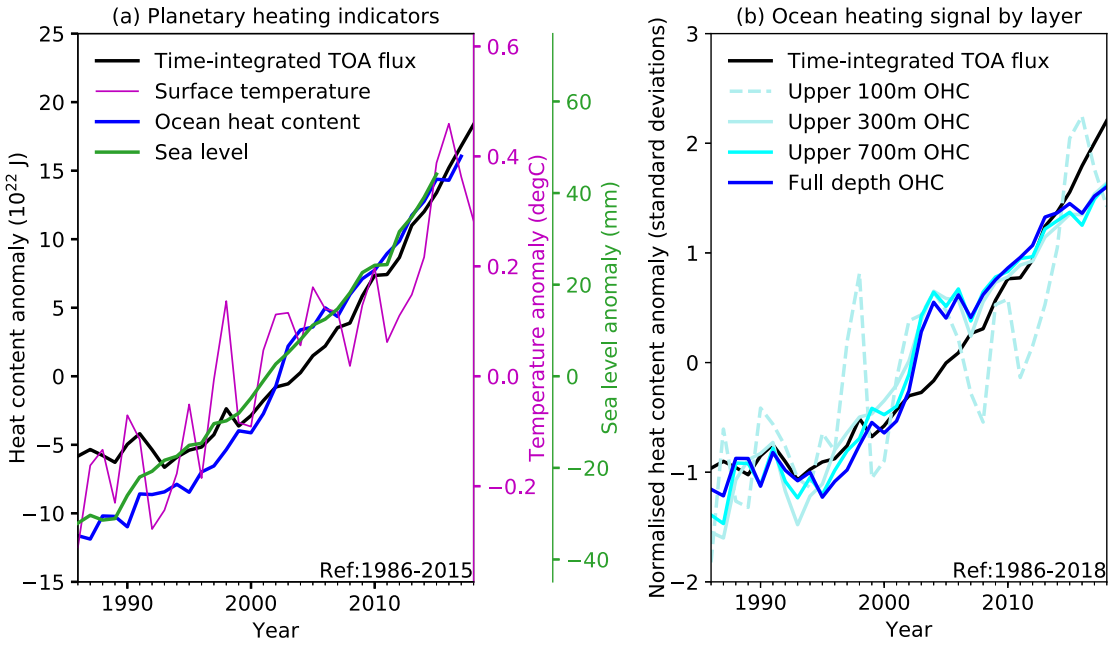

Figure 1. (a) Annual time series of planetary heat content anomaly estimated from time-integrated global mean radiative flux at the top of the atmosphere (EEI at TOA, based on Allan *et al* (2014) and Liu *et al* (2020)) in 10^{22} Joules [black curve, left axis]; global mean surface temperature (GMST, mean of three products as described in the text) in degrees Celsius [magenta curve, right axis]; global ocean heat content (GOHC, mean of six products as described in the text) in 10^{22} Joules [blue curve, left axis], global mean sea level (GMSL, Dangendorf *et al* 2019) in mm [green curve, second right axis]. Anomalies are relative to the mean over 1986–2015 (the period for which all variables are available). (b) Normalised anomaly in planetary heat content estimated from time-integrated EEI at TOA (as in panel (a) with normalisation) compared with the normalised MOSORA GOHC anomaly integrated from the surface to successively lower depth limits. If the lower boundary of a specified layer is not coincident with the lower boundary of a vertical level in the analysis, values are interpolated assuming homogenous temperature within each analysis level. Each time series is normalised by its annual standard deviation over 1986–2018 and anomalies are relative to the mean over the same period. Units are standard deviations.

Methods

A time series of GOHC (1986–2017) is calculated by taking the mean of the upper-2000 m GOHC estimates from six products. Four of these are previously published estimates: Levitus *et al* (2012), Ishii *et al* (2017), Cheng *et al* (2017b), and a combination of Domingues *et al* (2008) and Levitus *et al* (2012) for 0–700 m and 700–2000 m respectively (data from Cheng *et al* 2019). The remaining two estimates of upper-2000 m GOHC are calculated from global ocean temperature analyses: EN4 (Good *et al* 2013) and an updated version of MOSORA (after Smith *et al* 2015). The MOSORA contribution is the mean of a 10-member ensemble whose members use different global covariances to map *in situ* sub-surface ocean and sea surface temperature (SST) observations. To account for the estimated contribution to GOHC from depths below 2000 m, a constant warming rate of 0.065 W m^{-2} applied over Earth's surface area (Desbruyères *et al* 2016) is added to the GOHC time series. The quantification of uncertainty associated with GOHC estimates is an active research area. Uncertainty estimates are influenced by various historical circumstances and technical choices, including observational density, mapping methods and XBT bias corrections (e.g. Boyer *et al* 2016), and some of the variability in individual GOHC estimates is likely to be the result of residual sampling 'noise' (Abraham *et al* 2013, Smith *et al* 2015, Allison *et al* 2019). We address this issue by taking the mean of six GOHC products to reduce the noise in order to better estimate the signal of GOHC change and its variations.

Estimates of GMST are better constrained by the available observations than those of GOHC, but we follow a similar approach in deriving a time series of observed GMST (1986–2018) as the mean of three products: HadCRUT4 (Morice *et al* 2012), GISTEMP (Lenssen *et al* 2019) and NOAAGlobalTemp (Jones *et al* 1999). For the time series of EEI at TOA (1986–2018), we time-integrate the global mean radiative flux at the top of the atmosphere, which is based on Allan *et al* (2014) and Liu *et al* (2020). These TOA annual means are calculated for July-June so that the time-integrated TOA time series leads the state variables by 6 months (the flux is time-integrated up to the mid-point of the state variables' annual meaning window).

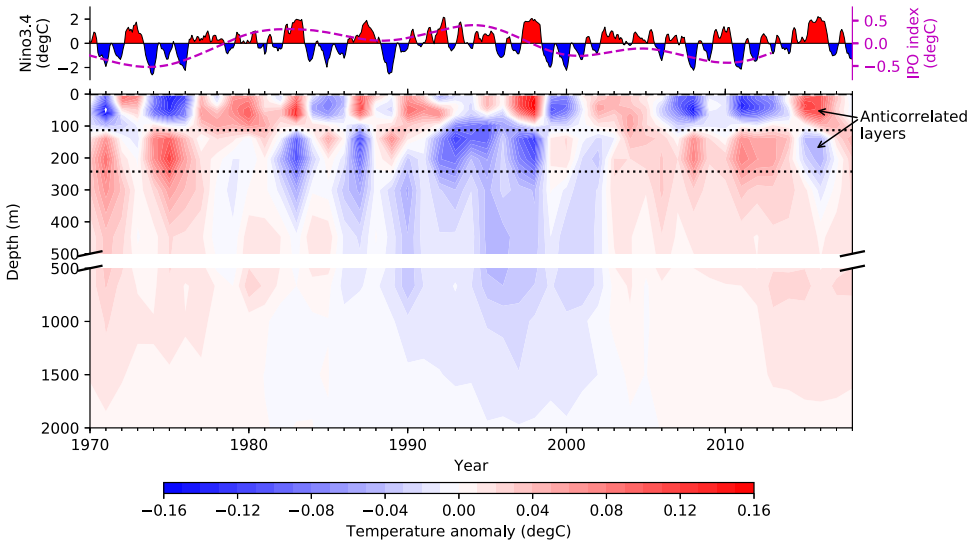

Figure 2. Global area mean annual ocean potential temperature anomaly as a function of depth (upper 2000 m) and time (1970–2018) from the MOSORA ensemble mean. Note the expanded vertical scale for the upper 500 m. The temperature time series have been linearly detrended to emphasise the variations superimposed upon the long-term warming signal. Dashed lines indicate the depth boundaries of the upper (0–113 m) and lower (113–243 m) layers used to calculate correlations. The precise location of these depth limits was determined by the position of the vertical grid boundaries in the analysis. The upper panel shows the monthly Nino3.4 SST anomaly time series calculated from HadISST (Rayner *et al* 2003) to indicate ENSO variability (left axis and red/blue shading) and a low-pass filtered tripole index to indicate decadal-scale IPO variability (data from Henley *et al* 2015; purple dashed line, right axis).

Results

The time series of planetary heat content anomaly inferred from time-integrated TOA flux reveals a clear and largely monotonic increase since the mid-1980s (figure 1(a)). In contrast, GMST exhibits considerable interannual and decadal variability. This variability is largely absent from GOHC and GMSL (which is closely linked to GOHC through thermal expansion); these 'full-ocean' variables more closely replicate the near-monotonic planetary heating inferred from TOA radiative flux measurements. It is clear that interannual trends in GMST are dominated by near-surface variability and are not representative of changes in planetary heat content.

As GOHC is integrated to deeper levels, the surface noise is diminished. This can be seen in figure 1(b), which compares the TOA-implied heating with the MOSORA GOHC anomalies over various depth ranges, with each time series normalised by its own standard deviation to emphasise the change signals captured in each layer. Upper 100 m GOHC contains significant interannual variability, with features similar to those seen in the GMST time series, reflecting the physical link between GMST and the heat content of the upper ocean mixed layer. However, even full-column GOHC estimates show some variability overlying the trend, some of which is likely artificial and may be attributed to residual noise associated with limited ocean sampling and changes in observing practices over time (Abraham *et al* 2013, Smith *et al* 2015, Allison *et al* 2019). The results in figure 1(b) suggest that on this ~30-year timescale, integrating GOHC to 300 m depth removes much of the near-surface noise and captures the character of the planetary heating signal. Integrating to deeper limits yields normalised signals that are similar to that of the upper 300 m. However, comparison of non-normalised time series (not shown) reveals that the deeper layers are important for capturing the magnitude of the long-term heating trend. In MOSORA, the 0–100 m layer captures 14% of the linear trend in the full-depth GOHC over 1986–2018, while the 0–300 m and 0–700 m layers capture 38% and 58% of the full-depth trend, respectively.

The depth structure of global mean ocean temperature variability (figure 2) reveals layers of anticorrelated anomalies above and below 100 m (Roemmich and Gilson 2011, Wijffels *et al* 2016) demonstrating that surface temperature variations are not representative of changes in deeper ocean heat content. These anticorrelated layers can be traced to vertical heat rearrangement in the Tropical Pacific associated with the El Niño Southern Oscillation (ENSO) on interannual timescales. Variations in the strength of the Pacific trade winds alter the subduction and convergence of heat in the equatorial thermocline and upwelling of cool water into the surface layer, changing the thermocline's east-west tilt (Roemmich and Gilson 2011). It can be seen in figure 2 that for a positive ENSO index (El Niño), the upper layer is anomalously warm and the lower layer anomalously cool, with a reversal of this pattern during negative events (La Niña). Global ocean temperature anomalies in the 0–100 m and 100–250 m layers are negatively correlated ($r = -0.36$). This anticorrelation between ocean layers is dominated by the Tropical Pacific; when this region (120°–280°E, 10° S-10° N) is excluded from the global mean

(not shown) the correlation becomes positive (r = +0.37), illustrating the impact of regional Tropical Pacific temperature variations on the global mean. In addition to the interannual variability within the upper few hundred metres, figure 2 also reveals clear decadal variability in sub-surface global mean ocean temperature that extends to 2000 m depth. The periods of sub-surface cooling (~1970–1995) and warming (~1995–2018) show close correspondence to observed epochs of positive and negative trends in the Interdecadal Pacific Oscillation (IPO) respectively, indicating that sub-surface ocean heat rearrangement also plays a role in global mean surface temperature variability on decadal timescales (England *et al* 2014, Meehl *et al* 2016). These modes of variability in the Pacific have been identified as important drivers of unforced variability in global mean surface temperature, but variations in the Atlantic Ocean and external forcings may also play a role (Dai *et al* 2015, Smith *et al* 2016).

Discussion

This observational analysis strongly supports previous findings based on climate model simulations, illustrating the de-coupling between EEI and GMST on decadal and shorter timescales. This de-coupling occurs primarily due to dynamic ocean heat rearrangement processes associated with climate variability in the Pacific. GOHC is largely independent of these internal rearrangements and remains strongly indicative of EEI on all timescales, exhibiting a much steadier rise than GMST. GMST is a fundamental quantity to monitor; it has a long and reliable historical record and it plays a central role in determining many important climate impacts. However, the implication here is that GOHC presents a more reliable basis for drawing insights on the evolving magnitude of EEI on decadal and shorter time periods. Our ability to track EEI for climate monitoring relies on a suite of complementary observation sources, including GOHC from sustained and improved ocean observations (e.g. the international Argo program, amongst others) as well as TOA measurements, and may also be enhanced through schemes that incorporate observations of GMSL in a physically consistent way (Meyssignac *et al* 2019). The striking agreement between the independent observational datasets of time-integrated net TOA flux, GOHC and GMSL (as well as multi-decadal trends in GMST) represents unequivocal evidence of ongoing planetary heating.

Acknowledgments

This work was supported by the Met Office Hadley Centre Climate Programme funded by BEIS and Defra. RPA's contribution was funded by the UK Natural Environment Research Council (NERC) SMURPHS project (NE/N006054/1) and the National Centre for Earth Observation (NE/RO16518/1).

ORCID iDs

Lesley C Allison https://orcid.org/0000-0002-9271-1197
Matthew D Palmer https://orcid.org/0000-0001-7422-198X
Richard P Allan https://orcid.org/0000-0003-0264-9447
Leon Hermanson https://orcid.org/0000-0002-1062-6731
Chunlei Liu https://orcid.org/0000-0002-6663-452X
Doug M Smith https://orcid.org/0000-0001-5708-694X

References

Abraham J P *et al* 2013 *Rev. Geophys.* **51** 450–83
Allan R P *et al* 2014 *Geophys. Res. Lett.* **41** 5588–97
Allison L C *et al* 2019 *Environ. Res. Lett.* **14** 084037
Boyer T 2016 *Journal of Climate* **29** 4817-4842
Cheng L *et al* 2017a *Eos* **98**
Cheng L *et al* 2017b *Sci. Adv.* **3** e1601545
Cheng L, Abraham J, Hausfather Z and Trenberth K E 2019 *Science* **363** 128–9
Dai A *et al* 2015 *Nature Climate Change* **5** 555-559
Dangendorf S *et al* 2019 *Nat. Clim. Chang.* **9** 705–10
Desbruyères D G, Purkey S G, McDonagh E L, Johnson G C and King B A 2016 *Geophys. Res. Lett.* **43** 10356–65
Domingues C M *et al* 2008 *Nature* **453** 1090–3
England M H *et al* 2014 *Nat. Clim. Chang.* **4** 222–7
Good S A, Martin M J and Rayner N A 2013 *J. Geophys. Res. Oceans* **118** 6704–16
Henley B J *et al* 2015 *Clim. Dyn.* **45** 3077–90
Ishii M *et al* 2017 *Sci. Online Lett. Atmos.* **13** 163–167

Johnson G C, Lyman J M and Loeb N G 2016 *Nat. Clim. Chang.* **6** 639–40
Jones P D, New M, Parker D E, Martin S and Rigor I G 1999 *Rev. Geophys.* **37** 173–99
Lenssen N *et al* 2019 *J. Geophys. Res. Atmos.* **124** 6307–26
Levitus S *et al* 2012 *Geophys. Res. Lett.* **39** L10603
Liu C *et al* 2020 *Clim. Dyn.* **10**
Medhaug I, Stolpe M B, Fischer E M and Knutti R 2017 *Nature* **545** 41–7
Meehl G A, Hu A, Santer B D and Xie S-P 2016 *Nat. Clim. Chang.* **6** 1005–8
Meyssignac B *et al* 2019 *Front. Mar. Sci.* **6** 432
Morice C P, Kennedy J J, Rayner N A and Jones P D 2012 *J. Geophys. Res.* **117** D08101
Palmer M D and McNeall D J 2014 *Environ. Res. Lett.* **9** 034016
Palmer M D, McNeall D J and Dunstone N J 2011 *Geophys. Res. Lett.* **38** L13707
Rayner N A *et al* 2003 *J. Geophys. Res.* **108** 4407
Roemmich D and Gilson J 2011 *Geophys. Res. Lett.* **38** L13606
Smith D M *et al* 2015 *Geophys. Res. Lett.* **42** 1205–13
Smith D M *et al* 2016 *Nat. Clim. Chang.* **6** 936–40
von Schuckmann K *et al* 2016 *Nat. Clim. Chang.* **6** 138–44
Wijffels S, Roemmich D, Monselesan D, Church J and Gilson J 2016 *Nat. Clim. Chang.* **6** 116–8